RSC Advances

PAPER

View Article Online
View Journal | View Issue

Cite this: *RSC Adv.*, 2014, **4**, 8597

Insight into the dynamic ligand exchange process involved in bipyridyl linked arene ruthenium metalla-rectangles†

Amine Garci,[a] Simon Marti,[b] Stefan Schürch[b] and Bruno Therrien*[a]

Received 20th November 2013
Accepted 17th January 2014

DOI: 10.1039/c3ra46859c

www.rsc.org/advances

The dynamic ligand exchange behavior of cationic arene ruthenium metalla-rectangles of the type $[(p\text{-cymene})_4Ru_4(OO\cap OO)_2(N\cap N)_2]^{4+}$ (OO∩OO = oxalato, 2,5-dioxydo-1,4-benzoquinonato, 5,8-dioxydo-1,4-naphthoquinonato; N∩N = 4,4′-bipyridine-H_8, 4,4′-bipyridine-D_8) has been studied in solution. The robustness of the rectangular architecture has been evidenced by NMR and ESI mass spectrometry. Thermodynamic and kinetic aspects of the ligand exchange process have been explored using $^1H/^2D$ isotope labeling of the 4,4′-bipyridine connectors. This study shows that ligand exchange does not proceed spontaneously for these metalla-assemblies, even at high temperature, unless an external stimulus is applied.

Introduction

The rules dictating the formation of supramolecular assemblies are well known, and a better understanding of the kinetic and thermodynamic aspects of the assembly–disassembly processes involved during the preparation of such supramolecular assemblies is essential for further chemical development.[1] In recent years, metalla-assemblies built from stable dinuclear arene ruthenium units and polypyridyl donor ligands have attracted a great deal of attention.[2] These systems have found applications as sensors,[3] as drug delivery vectors,[4] and as metal-based drugs.[5] However, little is known about the dynamic ligand exchange behavior of these systems in solution.

A fundamental facet of coordination-driven self-assemblies is the possible dynamic exchange process of the different building blocks involved.[6] Self-repairing, self-recognition, and self-rearrangement are frequently encountered in metalla-assemblies, and this dynamic behavior has been used to explain experimental results, even in many occasions without supporting experimental data. Indeed, examples that directly and quantitatively evidence the dynamic behavior of coordination-driven metalla-assemblies remain scarce.[7] This limited number of studies is partially due to the difficulty of finding an appropriate method of characterization. Among these methods, isotope labeling is potentially the easiest one to utilize; being compatible with NMR spectroscopy and mass spectrometry. However the preparation of isotope labeled compounds is not always trivial and can be expensive. Zheng and Stang have employed $^1H/^2D$ 4,4′-bipyridine ligands (bpy-H_8 and bpy-D_8) to study the dynamic ligand exchange behavior of platinum-based supramolecular metalla-cycles.[1a] A mixture of the homo-isotopic tetranuclear complexes $[(1,8\text{-bis}(trans\text{-}Pt(PEt_3)_2)\text{-anthracene})_2(\text{bpy-}H_8)_2]^{4+}$ and $[(1,8\text{-bis}(trans\text{-}Pt(PEt_3)_2)\text{anthracene})_2(\text{bpy-}D_8)_2]^{4+}$ was heated at 64 °C and the dynamic ligand exchange process was monitored for a prolonged period by ESI mass spectrometry. After several days, the reaction has reached equilibrium and a final 1 : 2 : 1 ratio between the homo-H_{16} : hetero-H_8/D_8 : homo-D_{16} metalla-rectangles was observed (Fig. 1). The dynamic exchange behavior of the Pt–N bonding assemblies was established, confirming the self-assembled nature of this system and the effectiveness of the $^1H/^2D$ isotope labeling methodology.

Another approach to study dynamic ligand exchange processes consists of adding to a well-defined metalla-assembly a competing ligand or competing metal ion, and after reorganization and equilibrium, to analyze the newly formed species.[8] Recently, Neogi and co-workers studied the response of defined heteroleptic metalla-supramolecular racks, rectangles, and trigonal prisms through the addition of pyridyl-based donor ligands. For example, excess of 1,2-di(pyridine-4-yl)ethyne forces a metalla-rectangle to alter into a rack architecture in solution.[9] Dynamic exchange processes can also be initiated by adding a competing metal ion as elegantly demonstrated by Hiraoka and Shionoya.[10] These kind of studies allow not only to better understand the dynamic behavior of these metalla-assemblies in solution but also to envisage new synthetic routes to construct varying structural motifs.

In this report, a combination of these two methods, addition of competing ligands and isotope labeling, has been used to

[a]*Institute of Chemistry, University of Neuchatel, Avenue de Bellevaux 51, CH-2000 Neuchatel, Switzerland. E-mail: bruno.therrien@unine.ch*

[b]*Department of Chemistry and Biochemistry, University of Berne, Freiestrasse 3, CH-3012 Berne, Switzerland*

† Electronic supplementary information (ESI) available. See DOI: 10.1039/c3ra46859c

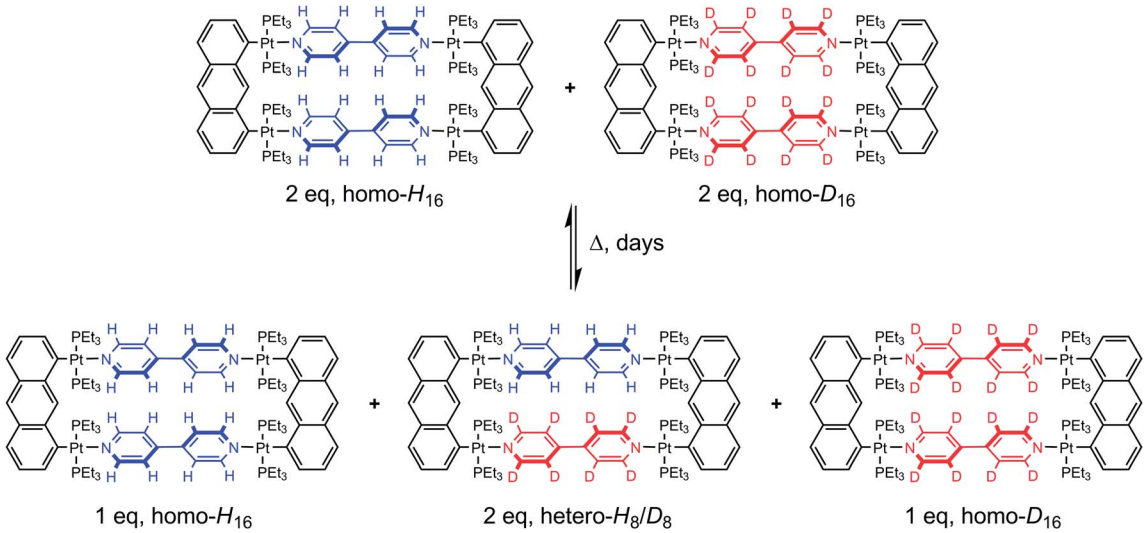

Fig. 1 Homo- and hetero-metalla-rectangles of the general formula $[(1,8\text{-bis}(trans\text{-Pt}(PEt_3)_2)\text{anthracene})_2(bpy)_2]^{4+}$ obtained after mixing equimolar amounts of the homo-H_{16} and homo-D_{16} metalla-rectangles, adapted from ref. 1*a*.

study the dynamic ligand exchange behavior of arene ruthenium metalla-rectangles containing bipyridyl linkers. Moreover, on the basis of quantitative mass spectral measurements and NMR spectroscopy, the kinetics of the stimuli-triggered ligand exchange process have been investigated.

Results and discussion

Six isotopic (isolated and purified) and three heteroisotopic (not isolated) arene ruthenium metalla-rectangles (see Fig. 2) of the general formula $[(p\text{-cymene})_4Ru_4(OO\cap OO)_2(N\cap N)_2]^{4+}$ (OO∩OO = oxalato, 2,5-dioxydo-1,4-benzoquinonato, 5,8-dioxydo-1,4-naphthoquinonato; N∩N = 4,4′-bipyridine-H_8, 4,4′-bipyridine-D_8) have been synthesized using the $^1H/^2D$ isotope-labeled 4,4′-bipyridine linkers. ESI-MS and ^1H NMR are used to observe and characterize the dynamic ligand exchange process operating in these cationic arene ruthenium metalla-assemblies.

The synthesis of the isotopic metalla-rectangles, $[(p\text{-cymene})_4Ru_4(OO\cap OO)_2(bpy\text{-}H_8)_2]^{4+}$ and $[(p\text{-cymene})_4Ru_4(OO\cap\Sigma OO)_2(bpy\text{-}D_8)_2]^{4+}$, has been performed following published methods using the corresponding dinuclear clips and bpy-H_8 or bpy-D_8, respectively.[11] On the other hand, two equivalents of the arene ruthenium metalla-clips $\{(p\text{-cymene})_2Ru_2(OO\cap OO)\}^{2+}$ react with a mixture of one equivalent of 4,4′-bipyridine-H_8 (bpy-H_8) and one equivalent of 4,4′-bipyridine-D_8 (bpy-D_8) to form a combination of the homo- and hetero-metalla-rectangles. The resulting mixture of the metalla-rectangles represents a statistical product distribution (theoretical value 1 : 2 : 1, homo-H_{16}, hetero-H_8/D_8, homo-D_{16}) (Fig. 3). In the case of the oxalato derivative, we were unable to confirm the formation of the hetero-H_8/D_8 metalla-rectangle; no peak corresponding to the intact arene ruthenium metalla-rectangles being observed by ESI-MS.

In order to observe a possible dynamic ligand exchange process between the homo-H_{16} and homo-D_{16} metalla-rectangles, as previously performed by Zheng and Stang with the metalla-rectangle $[(1,8\text{-bis}(trans\text{-Pt}(PEt_3)_2)\text{anthracene})_2(bpy)_2]^{4+}$ (Fig. 1),[1a] we first mixed in methanol-d_4 the protonated metalla-rectangles and their corresponding deuterated analogues in a 1 : 1 ratio (see Fig. S1–S3† for the ESI-MS spectra). The evolution of the mixtures was then followed for 14 days by ^1H NMR and ESI-MS (methanol-d_4, 40 °C) (Fig. S4 and S5†). From the ^1H NMR spectra we can notice in all cases the absence of signals associated with the uncoordinated 4,4′-bipyridine-H_8 ligand. For metalla-rectangles $[(p\text{-cymene})_4Ru_4(2,5\text{-dioxydo-1,4-benzoquinonato})_2(bpy)_2]^{4+}$ and $[(p\text{-cymene})_4Ru_4(5,8\text{-dioxydo-1,4-naphthoquinonato})_2(bpy)_2]^{4+}$,

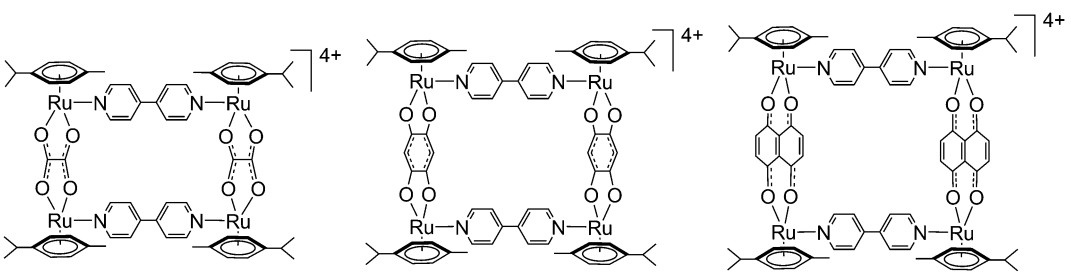

Fig. 2 Molecular structures of the cationic arene ruthenium metalla-rectangles.

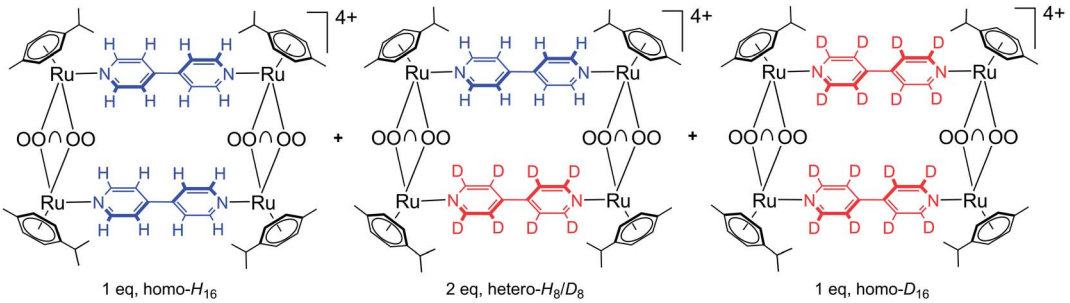

Fig. 3 Resulting statistical mixture of the homo- and hetero-metalla-rectangles (OO∩OO = oxalato, 2,5-dioxydo-1,4-benzoquinonato, 5,8-dioxydo-1,4-naphthoquinonato).

ESI-MS confirm that both protonated and deuterated metalla-rectangles are intact with no peak corresponding to the hetero-H_8/D_8 metalla-rectangles, thus suggesting no exchange of the 4,4′-bipyridine ligands. Selected peaks from the ESI-MS spectra of $[(p\text{-cymene})_4Ru_4(2,5\text{-dioxydo-1,4-benzoquinonato})_2(bpy)_2]^{4+}$ and $[(p\text{-cymene})_4Ru_4(5,8\text{-dioxydo-1,4-naphthoquinonato})_2(bpy)_2]^{4+}$, at the beginning, after 14 days, and from the mixed metalla-rectangles synthesized in a 1 : 2 : 1 ratio, are presented in Fig. 4 (calculated ESI-MS peaks are presented in Fig. S6†). The absence of the peaks corresponding to the hetero-derivatives $[M(H_8/D_8) - 2CF_3SO_3]^{2+}$ at m/z = 918 and 968, respectively, is clearly evidenced from these ESI-MS measurements (Fig. 4).

We also tried to initiate the exchange process by exposing the mixtures of the homo-metalla-rectangles under UV light and heating. After 24 hours in methanol-d_4 under UV irradiation (λ = 375 nm), we did not observe any exchange (^{1}H NMR and ESI-MS), only the apparition of free *p*-cymene molecules by ^{1}H NMR spectroscopy, suggesting decomposition of the arene ruthenium units. Similarly, after 48 hours at 65 °C in methanol-d_4, no evidence for the formation of the hetero-derivatives was observed, only slow decomposition of the metalla-rectangles.

The absence of spontaneous ligand exchange processes by simply mixing two isotopic metalla-rectangles forced us to modify our strategy. We decided to add to the homo-metalla-rectangles one equivalent of the free 4,4′-bipyridine ligand of the opposite labeling. First, we added one equivalent of 4,4′-bipyridine-H_8 to the smallest deuterated metalla-rectangle $[(p\text{-cymene})_4Ru_4(oxalato)_2(bpy\text{-}D_8)_2]^{4+}$ in methanol-d_4. Instantly, signals corresponding to coordinated bpy-H_8 appeared (H'_α and H'_β) in the ^{1}H NMR spectrum (Fig. 5). In parallel, a decrease in the intensity of the signals (H_α and H_β) of the free bpy-H_8 was observed. After 24 hours, the mixture had reached equilibrium and no more changes were observed in the ^{1}H NMR spectrum. The opposite experiment, addition of one equivalent of 4,4′-bipyridine-D_8 to metalla-rectangle $[(p\text{-cymene})_4Ru_4(oxalato)_2(bpy\text{-}H_8)_2]^{4+}$ in methanol-d_4, shows exactly the opposite behavior, which is in this case an increase of free bpy-H_8 signals and a decrease of the signals associated to the coordinated bpy-H_8 protons. The presence of free bpy-H_8 and a larger complex with coordinated bpy-H_8 ligand was confirmed by diffusion-ordered NMR spectroscopy (DOSY). The DOSY spectrum of the mixture obtained after addition of bpy-H_8 to $[(p\text{-cymene})_4Ru_4(oxalato)_2(bpy\text{-}D_8)_2]^{4+}$ in methanol-d_4 shows two species

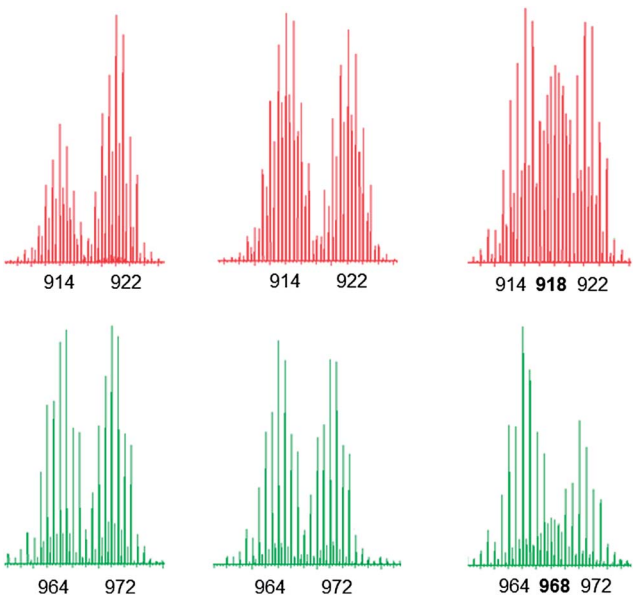

Fig. 4 Selected peaks ($[M - 2CF_3SO_3]^{2+}$) from the ESI-MS spectra of $[(p\text{-cymene})_4Ru_4(2,5\text{-dioxydo-1,4-benzoquinonato})_2(bpy)_2](CF_3SO_3)_4$ (top) and $[(p\text{-cymene})_4Ru_4(5,8\text{-dioxydo-1,4-naphthoquinonato})_2(bpy)_2](CF_3SO_3)_4$ (bottom), at the beginning after mixing the two homo-rectangles (left), after 14 days in solution at 40 °C (middle), and from the mixed metalla-rectangles synthesized in a 1 : 2 : 1 ratio (right).

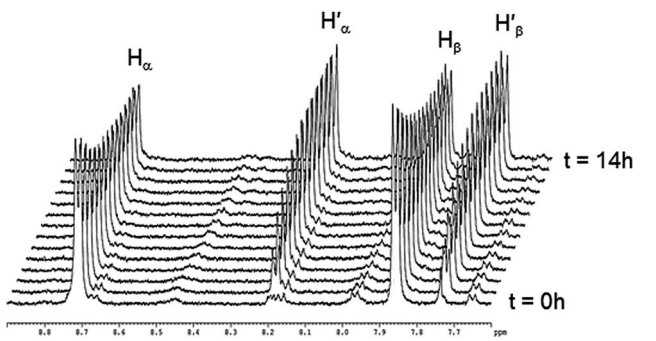

Fig. 5 Representative ^{1}H NMR spectra following the ligand exchange process with metalla-rectangle $[(p\text{-cymene})_4Ru_4(oxalato)_2(bpy\text{-}D_8)_2]^{4+}$ in methanol-d_4 (23 °C) upon addition of bpy-H_8.

(Fig. S7†), with a larger coefficient for the newly formed species, confirming the coordination of bpy-H_8 to ruthenium. To identify the nature of these new species, the two mixtures obtained after 24 hours were studied by ESI-MS. In both cases, the ESI mass spectra show two distinctive fragments incorporating both bpy ligands in their core (bpy-H_8 or bpy-D_8), a di-cationic fragment with peaks at $m/z = 786$ and 790, and a mono-cationic fragment with peaks at $m/z = 864$ and 872 (Fig. S8†). These fragments correspond to the species $[(p\text{-cymene})_4Ru_4(oxalato)_2(bpy) + 2CF_3SO_3]^{2+}$ and $[(p\text{-cymene})_2Ru_2(oxalato)(bpy) + CF_3SO_3]^{+}$, respectively.

Despite similar behavior, the kinetics of the ligand exchange processes before reaching equilibrium are different in these two experiments. The exchange process has been followed by ^{1}H NMR spectroscopy for 6 hours (Fig. 6), the rate of increase in the intensity of the coordinated bpy-H_8 signals in the first experiment is slower as compared to the rate of increase in intensity of the signals of free bpy-H_8 in the second experiment (Fig. 6a). This is due to the fact that in the first case, to exchange a Ru–N(bpy-D_8)–Ru bridge with a Ru–N(bpy-H_8)–Ru bridge, the disassembly of the metalla-rectangle $[(p\text{-cymene})_4Ru_4(oxalato)_2(bpy\text{-}D_8)_2]^{4+}$ has to take place first. In other words, two kinetic constants, a dissociative (k_d) and an associative (k_a) constants, are operating. In the second case (Fig. 6b), the appearance of free bpy-H_8 signals is due to the disassembly of the metalla-rectangle $[(p\text{-cymene})_4Ru_4(oxalato)_2(bpy\text{-}H_8)_2]^{4+}$, thus involving only the dissociative process.

In the case of the $[(p\text{-cymene})_4Ru_4(2,5\text{-dioxydo-}1,4\text{-benzoquinonato})_2(bpy)_2]^{4+}$ metalla-rectangle, a different behavior has been observed. In fact, when one equivalent of bpy-D_8 is added to $[(p\text{-cymene})_4Ru_4(2,5\text{-dioxydo-}1,4\text{-benzoquinonato})_2(bpy\text{-}H_8)_2]^{4+}$ in methanol-d_4 at 40 °C (Fig. S9†), the intensity of the signals corresponding to the protons of the coordinated bpy-H_8 (■) decreases, accompanied by the apparition of a signal at $\delta = 7.1$ ppm associated with free *p*-cymene (#). However, at room temperature, no clear exchange between the metalla-rectangles $[(p\text{-cymene})_4Ru_4(2,5\text{-dioxydo-}1,4\text{-benzoquinonato})_2(bpy)_2]^{4+}$ and 4,4′-bipyridine is observed (Fig. 7). Interestingly, when 1 equivalent of bpy-H_8 is added to $[(p\text{-cymene})_4Ru_4(2,5\text{-dioxydo-}1,4\text{-benzoquinonato})_2(bpy\text{-}D_8)_2]^{4+}$, only broad signals are observed in methanol-d_4 (Fig. 7a). This behavior suggests a slow assembly–disassembly and/or dissociative process of the bpy ligands on the NMR time scale. On the other hand, when bpy-D_8 is added to $[(p\text{-cymene})_4Ru_4(2,5\text{-dioxydo-}1,4\text{-benzoquinonato})_2(bpy\text{-}H_8)_2]^{4+}$ in methanol-d_4 at room temperature in a 1 : 1 ratio (Fig. 7b), the metalla-rectangle appears to be stable: The intensity of the signals attributed to the metalla-rectangle remaining unchanged for 6 hours.

In the case of $[(p\text{-cymene})_4Ru_4(5,8\text{-dioxydo-}1,4\text{-naphthoquinonato})_2(bpy)_2]^{4+}$, the dynamic ligand exchange process in methanol-d_4 upon addition of bpy is similar to that observed with the oxalato metalla-rectangles: a rapid exchange of the bpy ligands in solution after disassembly of the metalla-rectangle (Fig. 8). On the other hand, as observed for the oxalato and 2,5-dioxydo-1,4-benzoquinonato derivatives, the presence of free *p*-cymene molecules is not detected in solution, thus suggesting a more robust metalla-assembly. In the ^{1}H NMR spectrum, the protons associated with the 5,8-dioxydo-1,4-naphthoquinonato bridging ligand are observed as a singlet at $\delta = 7.24$ ppm. Interestingly, the ESI mass spectra of the solutions isolated after 6 hours reaction time show peaks corresponding to all metalla-rectangles at $m/z = 964$, 968 and 972, $[M(H_{16}) - 2CF_3SO_3]^{2+}$,

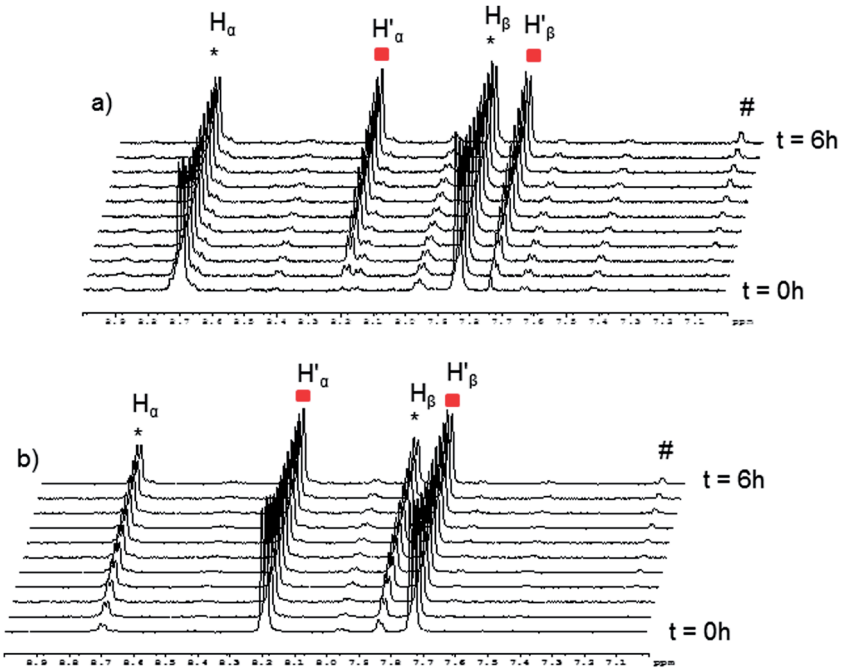

Fig. 6 Representative ^{1}H NMR spectra (6 hours) following the kinetic exchange between $[(p\text{-cymene})_4Ru_4(oxalato)_2(bpy)_2]^{4+}$ (■) and 4,4′-bipyridine (*) (methanol-d_4, 23 °C); (a) $[(p\text{-cymene})_4Ru_4(oxalato)_2(bpy\text{-}D_8)_2]^{4+}$ + bpy-H_8; (b) $[(p\text{-cymene})_4Ru_4(oxalato)_2(bpy\text{-}H_8)_2]^{4+}$ + bpy-D_8 (# = free *p*-cymene).

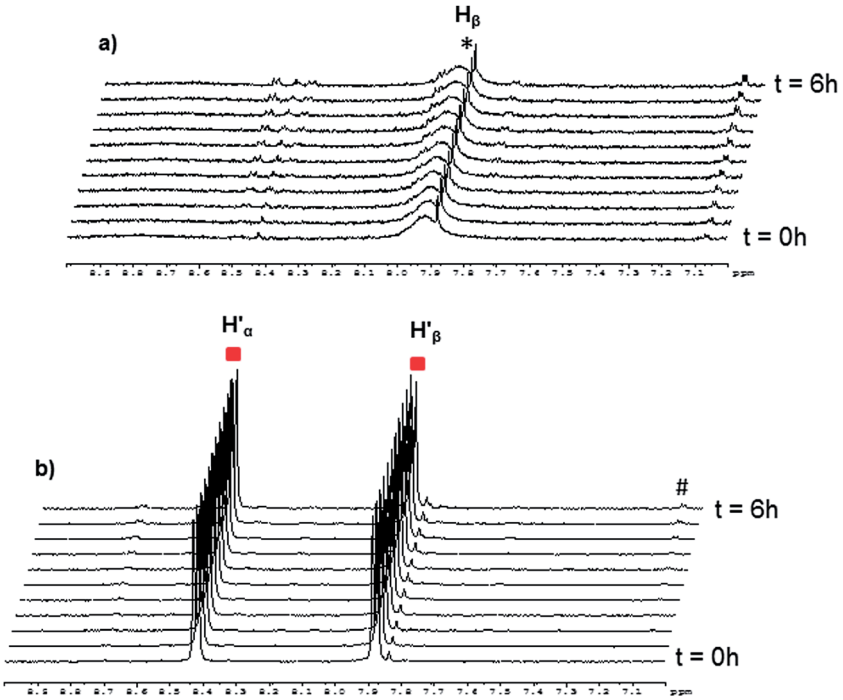

Fig. 7 Representative ^{1}H NMR spectra (6 hours) following the kinetic exchange between [(*p*-cymene)$_4$Ru$_4$(2,5-dioxydo-1,4-benzoquinonato)$_2$(bpy)$_2$]$^{4+}$ (■) and 4,4′-bipyridine (*) (methanol-d_4, 23 °C); (a) [(*p*-cymene)$_4$Ru$_4$(2,5-dioxydo-1,4-benzoquinonato)$_2$(bpy-D_8)$_2$]$^{4+}$ + bpy-H_8; (b) [(*p*-cymene)$_4$Ru$_4$(2,5-dioxydo-1,4-benzoquinonato)$_2$(bpy-H_8)$_2$]$^{4+}$ + bpy-D_8 (# = free *p*-cymene).

$[M(H_8/D_8) - 2CF_3SO_3]^{2+}$ and $[M(D_{16}) - 2CF_3SO_3]^{2+}$, respectively. The intensity of the peak corresponding to the mixed metalla-rectangle is nonetheless very low. Otherwise, peaks corresponding to fragments incorporating a bpy ligand in their core (bpy-H_8 or bpy-D_8) and {(*p*-cymene)$_2$Ru$_2$(5,8-dioxydo-1,4-naphthoquinonato)}$^{2+}$ are also observed; a di-cationic fragment with peaks at m/z = 886 and 890, and a mono-cationic fragment with peaks at m/z = 964 and 972. These fragments have been attributed to the two species [(*p*-cymene)$_4$Ru$_4$(5,8-dioxydo-1,4-naphthoquinonato)$_2$(bpy) + 2 CF_3SO_3]$^{2+}$ and [(*p*-cymene)$_2$Ru$_2$(5,8-dioxydo-1,4-naphthoquinonato)(bpy) + CF_3SO_3]$^+$, respectively (Fig. S10†).

As previously observed by NMR and mass spectrometry, addition of bpy to the metalla-rectangles produces several intermediates, thus obscuring the kinetics of the assembly–disassembly processes of the metalla-rectangles. Therefore, we chose to determine the initial rate of the reaction (V_0), when the initial concentrations of the metalla-rectangle and bpy are known and when the exchange processes follow a linear response (Fig. S11–S23†). These initial rates of the exchange processes at room temperature with a 1 : 1 and 1 : 10 ratio (metalla-rectangle : bpy) and at 40 °C with a 1 : 1 ratio are given in Table 1.

For the 2,5-dioxydo-1,4-benzoquinonato metalla-rectangle, the initial rate of the exchange process was only determined upon addition of bpy-D_8 to [(*p*-cymene)$_4$Ru$_4$(2,5-dioxydo-1,4-benzoquinonato)$_2$(bpy-H_8)$_2$]$^{4+}$ at 40 °C. The release of bpy-H_8 from the ruthenium atom is quite slow at this temperature and suggests a good stability of the metalla-rectangle. On the other hand, the initial rates of the exchange processes involving the other metalla-rectangles are faster. In both cases and as expected, the exchange process is more rapid when a 10-fold excess of bpy is added and when the temperature of the reaction is raised to 40 °C.

Finally, when the addition of one equivalent of the free 4,4′-bipyridine ligand to the six homo-metalla-rectangles is performed at −20 °C in methanol-d_4, no exchange occurs for several hours: All ^{1}H NMR spectra remaining identical, confirming the relative stability of these arene ruthenium metalla-rectangles in solution.

General remarks

The arene ruthenium metalla-rectangle [(*p*-cymene)Ru$_4$(OO∩ΣOO)$_2$(bpy-H_8)$_2$](CF$_3$SO$_3$)$_4$ (OO∩OO = oxalato, 2,5-dioxydo-1,4-benzoquinonato, 5,8-dioxydo-1,4-naphthoquinonato) were prepared according to published methods.[11] 4,4′-Bipyridine-D_8 (bpy-D_8) was purchased from Aldrich (purity 98 atom % D), while all other reagents were purchased from Alfa Aesar or Aldrich. The ^{1}H and ^{13}C{^{1}H} NMR spectra were recorded on Bruker Avance II 400 spectrometers using the residual protonated solvent or TMS as internal standard. Infrared spectra were recorded as KBr pellets on a Perkin-Elmer FTIR 1720 X spectrometer. Electrospray and nano-electrospray mass spectra were recorded in the positive-ion mode on a LCQ ion trap (Thermo Finnigan) and a LTQ Orbitrap XL mass spectrometer (Thermo Scientific), respectively. UV-visible absorption spectra were recorded on a Perkin Elmer UV/Vis spectrophotometer Lambda 24 (10^{-5} M in CH_2Cl_2).

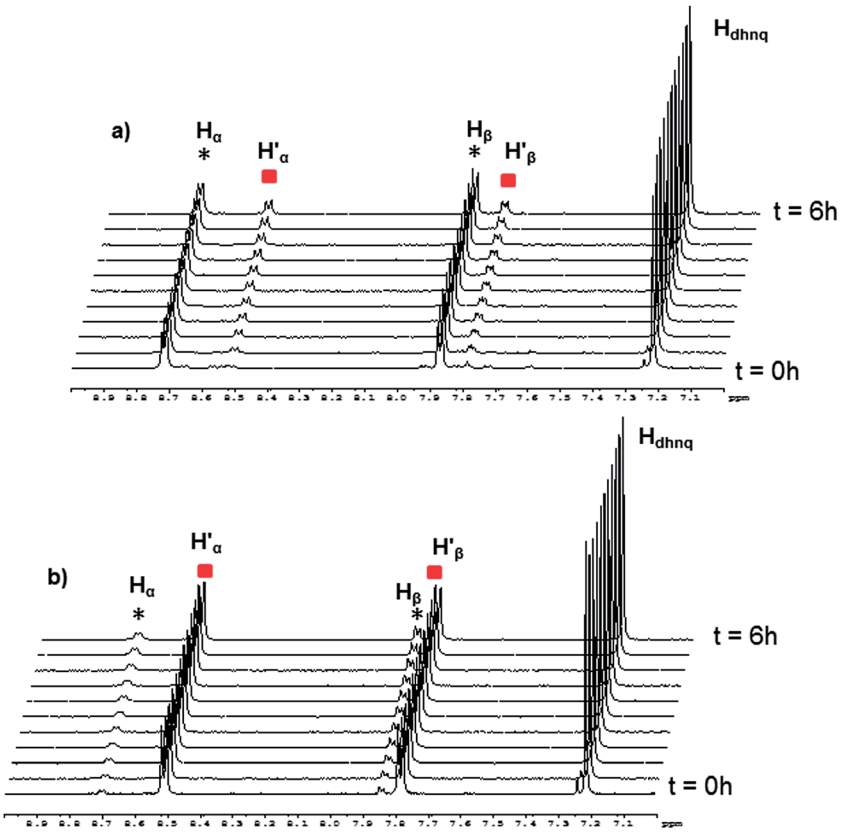

Fig. 8 Representative ^{1}H NMR spectra (6 hours) following the kinetic exchange between [(*p*-cymene)$_4$Ru$_4$(5,8-dioxydo-1,4-naphthoquinonato)$_2$(bpy)$_2$]$^{4+}$ (■) and 4,4′-bipyridine (*) (methanol-d_4, 23 °C); (a) [(*p*-cymene)$_4$Ru$_4$(5,8-dioxydo-1,4-naphthoquinonato)$_2$(bpy-D_8)$_2$]$^{4+}$ + bpy-H_8; (b) [(*p*-cymene)$_4$Ru$_4$(5,8-dioxydo-1,4-naphthoquinonato)$_2$(bpy-H_8)$_2$]$^{4+}$ + bpy-D_8.

Table 1 Initial rates of the exchange processes between the homo-metalla-rectangles and the free 4,4′-bipyridine of the opposite labeling, (homo-H_{16} + bpy-D_8 = $V_{0'}$, homo-D_{16} + bpy-H_8 = $V_{0''}$)

	Initial rate × 10^{-5} $V_{0'}$ (mol L^{-1} min^{-1})			Initial rate × 10^{-5} $V_{0''}$ (mol L^{-1} min^{-1})		
Metalla-rectangle [(*p*-cymene)$_4$Ru$_4$-(OO∩OO)$_2$(bpy)$_2$]$^{4+}$OO∩OO =	1 eq.	10 eq.	1 eq. (40 °C)	1 eq.	10 eq.	1 eq. (40 °C)
Oxalato	5.8	14.1	20.4	3.8	7.2	14.8
2,5-Dioxydo-1,4-benzoquinonato	—	—	1.9	—	—	—
5,8-Dioxydo-1,4-naphthoquinonato	4.7	8.2	7.1	4.4	9.6	17.4

General synthetic method for the isotopic metalla-rectangles of the general formula [(*p*-cymene)Ru$_4$(OO∩OO)$_2$(bpy-D_8)$_2$](CF$_3$SO$_3$)$_4$

A mixture of the dinuclear clip [(*p*-cymene)$_2$Ru$_2$(OO∩OO)Cl$_2$] (OO∩OO = oxalato, 2,5-dioxydo-1,4-benzoquinonato, 5,8-dioxydo-1,4-naphthoquinonato) (0.16 mmol) and 2 eq. of AgCF$_3$SO$_3$ (0.32 mmol) in methanol (20 mL) was stirred at room temperature for 2 h and the solution was filtered to remove AgCl. To the filtrate, the corresponding 4,4′-bipyridine-D_8 (bpy-D_8) (0.16 mmol) was added. The mixture was stirred at room temperature for 24 h, and the solvent removed under vacuum. The residue was dissolved in dichloromethane (20 mL), the extract filtered and concentrated (3 mL), and diethyl ether was slowly added to initiate precipitation of the product as a dark orange or red solid.

[(*p*-Cymene)$_4$Ru$_4$(oxalato)$_2$(bpy-D_8)$_2$](CF$_3$SO$_3$)$_4$. Orange solid, yield: 0.052 mmol (65%). ^{1}H NMR (400 MHz, methanol-d_4): δ (ppm), 5.96(d, 8H, $^{3}J_{H-H}$ = 6.2 Hz, C$H_{p\text{-cym}}$), 5.78 (d, 8H, $^{3}J_{H-H}$ = 6.2 Hz, C$H_{p\text{-cym}}$), 2.95 (sept, 4H, $^{3}J_{H-H}$ = 6.9 Hz, CH(CH$_3$)$_2$), 2.23 (s, 12H, CH_3), 1.39 (d, 24H, $^{3}J_{H-H}$ = 6.9 Hz, CH(CH_3)$_2$). ^{13}C{^{1}H} NMR (100 MHz, methanol-d_4): δ (ppm) 172.5 (*C*=O), 149.27 (*C*$_{bpy}$), 142.12 (*C*$_{bpy}$), 125.6 (*C*$_{bpy}$), 103.97 (*C*$_{p\text{-cym}}$), 99.13 (*C*$_{p\text{-cym}}$), 83.61 (*C*H$_{p\text{-cym}}$), 82.99 (*C*H$_{p\text{-cym}}$), 32.48 (*C*H(CH$_3$)$_2$), 22.47 (CH(*C*H$_3$)$_2$), 18.02 (*C*H$_3$). IR (cm^{-1}): 3077 (w, CH$_{p\text{-cym}}$), 1634(s, C=O), 1578 (s, C=C$_{bpy}$), 1259 (s, CF$_3$). UV-visible: (1.0 × 10^{-5}

M, CH_2Cl_2, 298 K): λ_{max} 241 nm (ε = 29 371 M^{-1} cm^{-1}), 311 nm (ε = 25 684 M^{-1} cm^{-1}). ESI-MS: 790 [M − bpy − $2CF_3SO_3$]$^{2+}$, 872 [1/2 M − CF_3SO_3]$^{1+}$, 708 [1/2 M − bpy − CF_3SO_3]$^{1+}$.

[(*p*-Cymene)$_4$Ru$_4$(2,5-dioxydo-1,4-benzoquinonato)$_2$(bpy-D_8)$_2$](CF$_3$SO$_3$)$_4$. Red solid, yield: 0.053 mmol (66%). ^{1}H NMR (400 MHz, methanol-d_4): δ (ppm), 6.02 (d, 8H, $^3J_{H-H}$ = 6.4 Hz, C$H_{p\text{-cym}}$), 5.80 (d, 8H, $^3J_{H-H}$ = 6.4 Hz, C$H_{p\text{-cym}}$), 5.77 (s, 8H, CH_{dhbq}), 2.87 (sep, 4H, $^3J_{H-H}$ = 6.9 Hz, CH(CH$_3$)$_2$), 2.17 (s, 12H, CH_3), 1.35 (d, 24H, $^3J_{H-H}$ = 6.9 Hz, CH(CH_3)$_2$). ^{13}C{^{1}H} NMR (100 MHz, methanol-d_4): δ (ppm) 185.7 (*C*=O), 146.7 (C_{bpy}), 144.7 (C_{bpy}), 123.6 (C_{bpy}), 105.56 ($C_{p\text{-cym}}$), 103.00 (*C*H$_{dhbq}$), 100.35 ($C_{p\text{-cym}}$), 85.07 (*C*H$_{p\text{-cym}}$), 83.55 (*C*H$_{p\text{-cym}}$), 32.73 (*C*H(CH$_3$)$_2$), 22.68 (CH(*C*H$_3$)$_2$), 18.28 (*C*H$_3$). IR (cm^{-1}): 3066 (w, CH$_{p\text{-cym}}$), 1580 (s, C=C$_{bpy}$), 1527 (s, C=O), 1258 (s, CF_3). UV-visible: (1.0 × 10^{-5} M, CH_2Cl_2, 298 K): λ_{max} 308 nm (ε = 45 981 M^{-1} cm^{-1}), 491 nm (ε = 30 945 M^{-1} cm^{-1}). ESI-MS: 922 [M − $2CF_3SO_3$]$^{2+}$.

[(*p*-Cymene)$_4$Ru$_4$(5,8-dioxydo-1,4-naphthoquinonato)$_2$(bpy-D_8)$_2$](CF$_3$SO$_3$)$_4$. Dark green solid, yield: 0.053 mmol (66%). ^{1}H NMR (400 MHz, methanol-d_4): δ (ppm), 7.24 (s, 8H, CH_{dhnq}), 5.86 (d, 8H, $^3J_{H-H}$ = 6.4 Hz, C$H_{p\text{-cym}}$), 5.63 (d, 8H, $^3J_{H-H}$ = 6.4 Hz, C$H_{p\text{-cym}}$), 2.83 (sep, 4H, $^3J_{H-H}$ = 7 Hz, CH(CH$_3$)$_2$), 2.17 (s, 12H, CH_3), 1.35 (d, 24H, $^3J_{H-H}$ = 7 Hz, CH(CH_3)$_2$). ^{13}C{1H} NMR (100 MHz, methanol-d_4): δ (ppm) 172.26 (*C*=O), 153.49 (C_{bpy}), 146.55 (C_{bpy}) 138.62 (*C*H$_{dhnq}$), 124.15 (C_{bpy}), 112.58 (*C*H$_{dhnq}$), 105.04 ($C_{p\text{-cym}}$), 101.24 ($C_{p\text{-cym}}$), 85.96 (*C*H$_{p\text{-cym}}$), 84.03 (*C*H$_{p\text{-cym}}$), 31.98 (*C*H(CH$_3$)$_2$), 22.46 (CH(*C*H$_3$)$_2$), 17.31 (*C*H$_3$). IR (cm^{-1}): 3066 (w, CH$_{p\text{-cym}}$), 1578 (s, C=C$_{bpy}$), 1536 (s, C=O), 1259 (s, CF_3). UV-visible: (1.0 × 10^{-5} M, CH_2Cl_2, 298 K): λ_{max} 317 nm (ε = 33 470 M^{-1} cm^{-1}), 433 nm (ε = 17 300 M^{-1} cm^{-1}), 642 nm (ε = 1300 M^{-1} cm^{-1}), 695 nm (ε = 2863 M^{-1} cm^{-1}). ESI-MS: 972 [M − CF_3SO_3]$^{2+}$.

General synthetic method for the heterotopic metalla-rectangles of the general formula [(*p*-cymene)Ru$_4$(OO∩OO)$_2$(bpy-H_8)(bpy-D_8)](CF$_3$SO$_3$)$_4$

A mixture of the dinuclear clip [(*p*-cymene)$_2$Ru$_2$(OO∩OO)Cl$_2$] (OO∩OO = oxalato, 2,5-dioxydo-1,4-benzoquinonato, 5,8-dioxydo-1,4-naphthoquinonato) (0.16 mmol) and 2 eq. of $AgCF_3SO_3$ (0.32 mmol) in methanol (20 mL) was stirred at room temperature for 2 h and the solution was filtered to remove AgCl. To the filtrate, a mixture of bpy-H_8 and bpy-D_8 (0.08 mmol + 0.08 mmol) was added. The mixture was stirred at room temperature for 24 h, and the solvent removed under vacuum. Then, the residue was dissolved in dichloromethane (20 mL), the extract filtered and concentrated (3 mL), and diethyl ether was slowly added to initiate precipitation of the product as a dark orange or red solids: The average yield of the obtained metalla-rectangle mixtures being 63%.

All NMR data are consistent with the formation of the mixed metalla-rectangles (Fig. 3), however, no chemical shifts of the protons between the ^{1}H/^{2}D species are observed, only the integration being consistent with the expected mixtures between the homo- and hetero-metalla-rectangles.

[(*p*-Cymene)$_4$Ru$_4$(oxalato)$_2$(bpy-H_8)(bpy-D_8)](CF$_3$SO$_3$)$_4$. Orange solid. ESI-MS: 786 [M(D_8/H_8) − (bpy-D_8) − $2CF_3SO_3$]$^{2+}$, 790 [M(D_8/H_8) − (bpy-H_8) − $2CF_3SO_3$]$^{2+}$, 864 [1/2 M(D_8/H_8) − CF_3SO_3]$^{1+}$, 872 [1/2 M(D_8/H_8) − CF_3SO_3]$^{1+}$.

[(*p*-Cymene)$_4$Ru$_4$(2,5-dioxydo-1,4-benzoquinonato)$_2$(bpy-H_8)(bpy-D_8)](CF$_3$SO$_3$)$_4$. Red solid. ESI-MS: 836 [M(D_8/H_8) − (bpy-D_8) − $2CF_3SO_3$]$^{2+}$, 840 [M(D_8/H_8) − (bpy-H_8) − $2CF_3SO_3$]$^{2+}$, 918 [M(D_8/H_8) − $2CF_3SO_3$]$^{2+}$.

[(*p*-Cymene)$_4$Ru$_4$(5,8-dioxydo-1,4-naphthoquinonato)$_2$(bpy-H_8)(bpy-D_8)](CF$_3$SO$_3$)$_4$. Dark green solid. ESI-MS: 886 [M(D_8/H_8) − (bpy-D_8) − $2CF_3SO_3$]$^{2+}$, 890 [M(D_8/H_8) − (bpy-H_8) − $2CF_3SO_3$]$^{2+}$, 968 [M(D_8/H_8) − $2CF_3SO_3$]$^{2+}$.

References

1 (*a*) Y. R. Zheng and P. J. Stang, *J. Am. Chem. Soc.*, 2009, **131**, 3487; (*b*) M. D. Pluth and K. N. Raymond, *Chem. Soc. Rev.*, 2007, **36**, 161; (*c*) J. M. Lehn, *Chem. Soc. Rev.*, 2007, **36**, 151.

2 (*a*) K. Severin, *Chem. Commun.*, 2006, 3859; (*b*) B. Therrien, *Eur. J. Inorg. Chem.*, 2009, 2445; (*c*) Y.-F. Han, H. Li and G.-X. Jin, *Chem. Commun.*, 2010, **46**, 6879; (*d*) B. Therrien, *Top. Curr. Chem.*, 2012, **319**, 35; (*e*) A. Mishra, S. C. Kang and K.-W. Chi, *Eur. J. Inorg. Chem.*, 2013, 5222; (*f*) T. R. Cook, V. Vajpayee, M. H. Lee, P. J. Stang and K.-W. Chi, *Acc. Chem. Res.*, 2013, **46**, 2464; (*g*) G. Süss-Fink, *J. Organomet. Chem.*, 2014, **751**, 2; (*h*) A. K. Singh, D. S. Pandey, Q. Xu and P. Braunstein, *Coord. Chem. Rev.*, 2014, DOI: 10.1016/j.ccr.2013.09.009.

3 (*a*) M. Wang, V. Vajpayee, S. Shanmugaraju, Y. R. Zheng, Z. Zhao, H. Kim, P. S. Mukherjee, K.-W. Chi and P. J. Stang, *Inorg. Chem.*, 2011, **50**, 1506; (*b*) B. Kilbas, S. Mirtschin, R. Scopelliti and K. Severin, *Chem. Sci.*, 2012, **3**, 701.

4 (*a*) B. Therrien, G. Süss-Fink, P. Govindaswamy, A. K. Renfrew and P. Dyson, *Angew. Chem., Int. Ed.*, 2008, **47**, 3773; (*b*) O. Zava, J. Mattsson, B. Therrien and P. J. Dyson, *Chem. – Eur. J.*, 2010, **16**, 1428; (*c*) F. Schmitt, J. Freudenreich, N. P. E. Barry, L. Juillerat-Jeanneret, G. Süss-Fink and B. Therrien, *J. Am. Chem. Soc.*, 2012, **134**, 754.

5 (*a*) F. Linares, M. A. Galindo, S. Galli, M. A. Romero, J. A. R. Navarro and E. Barea, *Inorg. Chem.*, 2009, **48**, 7413; (*b*) N. P. E. Barry, F. Edafe and B. Therrien, *Dalton Trans.*, 2011, **40**, 7172; (*c*) A. Dubey, J. W. Min, H. J. Koo, H. Kim, T. R. Cook, S. C. Kang, P. J. Stang and K.-W. Chi, *Chem. – Eur. J.*, 2013, **19**, 11622; (*d*) G. Gupta, B. S. Murray, P. J. Dyson and B. Therrien, *Materials*, 2013, **6**, 5352.

6 (*a*) K. Nakabayashi, M. Kawano, M. Yoshizawa, S. Ohkoshi and M. Fujita, *J. Am. Chem. Soc.*, 2004, **126**, 16694; (*b*) A. V. Davis and K. N. Raymond, *J. Am. Chem. Soc.*, 2005, **127**, 7912; (*c*) M. Kawano, Y. Kobayashi, T. Ozeki and M. Fujita, *J. Am. Chem. Soc.*, 2006, **128**, 6558.

7 (*a*) M. D. Levin and P. J. Stang, *J. Am. Chem. Soc.*, 2000, **122**, 7428; (*b*) A. Hori, A. Akasaka, K. Biradha, S. Sakamoto, K. Yamaguchi and M. Fujita, *Angew. Chem., Int. Ed.*, 2002, **41**, 3269; (*c*) T. Yamamoto, A. M. Arif and P. J. Stang, *J. Am. Chem. Soc.*, 2003, **125**, 12309; (*d*) A. V. Davis, D. Fiedler, G. Seeber, A. Zahl, R. Van Eldik and K. N. Raymond, *J. Am. Chem. Soc.*, 2006, **128**, 1324; (*e*) M. D. Pluth and K. N. Raymond, *Chem. Soc. Rev.*, 2006, **36**, 161;

(*f*) C. G. Claessens, M. J. Vicente-Arana and T. Torres, *Chem. Commun.*, 2008, 6378.
8 J. R. Li and H. C. Zhou, *Nat. Chem.*, 2010, **2**, 893.
9 S. Neogi, Y. Lorenz, M. Engeser, D. Samanta and M. Schmittel, *Inorg. Chem.*, 2013, **52**, 6975.
10 S. Hiraoka, Y. Sakata and M. Shionoya, *J. Am. Chem. Soc.*, 2008, **130**, 10058.
11 (*a*) H. Yan, G. Süss-Fink, A. Neels and H. Stoeckli-Evans, *J. Chem. Soc., Dalton Trans.*, 1997, 4345; (*b*) J. Mattsson, P. Govindaswamy, A. K. Renfrew, P. J. Dyson, P. Štěpnička, G. Süss-Fink and B. Therrien, *Organometallics*, 2009, **28**, 4350; (*c*) N. P. E. Barry, J. Furrer, J. Freudenreich, G. Süss-Fink and B. Therrien, *Eur. J. Inorg. Chem.*, 2010, 725.